

Using deep Residual Network to search for galaxy-Ly α emitter lens candidates based on spectroscopic-selection

Rui Li^{1,2,4*}, Yiping Shu^{5,6†}, Jianlin Su⁷, Haicheng Feng^{1,2,3,4}, Jiancheng Wang^{1,2,3,4‡}

¹ Yunnan Observatories, Chinese Academy of Sciences, 396 Yangfangwang, Guandu District, Kunming, 650216, P. R. China

² University of Chinese Academy of Sciences, Beijing, 100049, P. R. China

³ Center for Astronomical Mega-Science, Chinese Academy of Sciences, 20A Datun Road, Chaoyang District, Beijing, 100012, P. R. China

⁴ Key Laboratory for the Structure and Evolution of Celestial Objects, Chinese Academy of Sciences, 396 Yangfangwang, Guandu District, Kunming, 650216, P. R. China

⁵ Purple Mountain Observatory, Chinese Academy of Sciences, 2 West Beijing Road, Nanjing, Jiangsu, 210008, China

⁶ Institute of Astronomy, University of Cambridge, Madingley Road, Cambridge CB3 0HA, UK

⁷ School of Mathematics, Sun Yat-sen University, Guangzhou, China

Accepted XXX. Received YYY; in original form ZZZ

ABSTRACT

More than one hundred galaxy-scale strong gravitational lens systems have been found by searching for the emission lines coming from galaxies with redshift higher than the lens galaxies. Based on this spectroscopic-selection method, we introduce the deep Residual Network (ResNet, a kind of deep Convolutional Neural Networks) to search for the galaxy-Ly α emitter (LAE) lens candidates by recognizing the Ly α emissions coming from high redshift ($2 < z < 3$) galaxies in the spectra of early-type galaxies (ETGs) at middle ($z \sim 0.5$) redshift. The spectra of the ETGs come from the Data Release 12 (DR12) of the Baryon Oscillation Spectroscopic Survey (BOSS) of the Sloan Digital Sky Survey III (SDSS-III). In this paper, we first build a 28 layers ResNet model, and then artificially synthesize 150,000 training spectra, including 140,000 spectra without Ly α emissions and 10,000 with Ly α emissions, to train the network. After 25 epochs training, we obtain a near-perfect test accuracy at 99.54% in our model, and the corresponding loss is 0.0028. We finally apply our ResNet model to our predictive data with 174 known lens candidates. We obtain 1232 hits including 161 (92.5% discovery rate) of the 174 known candidates. Apart from the hits found in other works, our ResNet model also find 536 new hits. We then perform several subsequent selections to these 536 hits and present 6 most believable lens candidates.

Key words: gravitational lensing: strong - galaxies: elliptical - galaxies:structure

1 INTRODUCTION

Galaxy-scale strong gravitational lenses, which can provide very tight constraints on the projected mass of the lens galaxies, are not only available probes to study the structures, the formation and evolution of galaxies (e.g., Koopmans et al. (2006); Auger et al. (2010); Sonnenfeld et al. (2013), Bolton et al. (2012)), but also a crucial technique to study cosmology, for example (Suyu et al. 2013). Additionally, gravitational lenses could act as natural telescopes and give us magnified views of the background objects, which could help us to study the ce-

lestial body in the distant universe(e.g., Impellizzeri et al. (2008); Swinbank et al. (2009); Treu et al. (2015).

Several methods have been used to search for the galaxy-scale strong gravitational lenses. Among them, an efficient method is searching for the arc-like morphological feature of the strong lens systems (Lenzen et al. 2004; Horesh et al. 2005; Seidel & Bartelmann 2007; Kubo & Dell’Antonio 2008; More et al. 2012). In order to find some strong lens systems in a great deal of targets, Gavazzi et al. (2014) subtracted the light of the central galaxies using multi-band images and then searched for the arc-like shapes in the residual images. Another modified work was done by Joseph et al. (2014), they successfully used the Principal Component Analysis (PCA) to subtract the light of the foreground galaxies, and then searched for gravitational lens feature in the resulting residual images.

* E-mail: lirui@ynao.ac.cn

† E-mail: yiping.shu@pmo.ac.cn

‡ E-mail: jcwang@ynao.ac.cn

They pointed out that the PCA-based galaxy subtraction algorithm performed better than the traditional model fitting method (Gavazzi et al. 2014).

Besides the method of morphological recognition, Warren et al. (1996) proposed a spectroscopic-selection technique to search for strong lens systems. This technique identifies lens candidates by looking for compound spectra. As shown in Figure 3, the left panel is a compound spectrum of an identified lensing system (SDSSJ 1110+2808, Shu et al. 2016b). The foreground galaxy of this lens system is an early-type galaxy (ETG, $z \sim 0.6073$) and its spectrum has no emissions between 3800Å and 5000Å. However, near the wavelength of 4150Å we find an emission which in fact is a Ly α line from a Ly α emitter (LAE). The LAE lies close to the line of sight of the ETG and at the redshift of $z = 2.3999$, which indicate that the light from the LAE is likely to be deflected by the foreground ETG and thus several images of the background LAE may occur around the foreground ETG. Further detail description of the spectroscopic-selection technique can be found in Bolton et al. (2004). In general, this technique is used for searching the spectrum with emissions from a background source, and then the high-resolution images are used to confirm the lens properties.

Several galaxy-scale strong lens surveys have been made with above spectroscopic-selection technique, such as the Sloan Lens ACS (SLACS, Bolton et al. 2006, 2008) survey, the Sloan WFC Edge-on Late-type Lens Survey (SWELLS, Treu et al. 2011), the Baryon Oscillation Spectroscopic Survey (BOSS) Emission-Line Lens Survey (BELLS, Bolton et al. 2012), the SLACS for the Masses (S4TM, Shu et al. 2015) and the BELLS for the GALaxy-Ly α EmittER sYstems (BELLS GALLERY, Shu et al. 2016b) survey. These surveys have found more than one hundred galaxy-galaxy strong gravitational lenses and have generated numerous substantial studies about the structures, the formation and evolution of ETGs (Koopmans et al. 2006; Auger et al. 2009; Bolton et al. 2012; Shu et al. 2015). Recently, using a similar technique, Meyer et al. (2017) have found a sample of 9 secure QSO-Galaxy lens candidates, presenting the potential application of the spectroscopic-selection technique in finding QSOs Lens. So far, this spectroscopic-selection technique is the most efficient method. However, the speed of the codes is not fast enough, especially in the coming age of the big data of astronomy.

Several years ago, the Convolutional Neural Networks (CNNs) which is a kind of machine learning algorithm particularly suitable for image recognition tasks, have been applied in astronomy. The first application of CNNs is the spectral classification of the tenth data release (DR10) of the Sloan Digital Sky Survey (SDSS). Hála (2014) applied his CNNs model on more than 60000 spectra of SDSS and yielded success rate of nearly 95%. His work conclusively proved great potential of CNNs and deep learning methods in astrophysics. Later, the CNNs have been applied to many other works, such as the morphological classification of SDSS galaxies (Dieleman, Willett, & Dambre 2015), the photometric redshifts estimation of SDSS galaxies (Hoyle 2016) and the star/galaxy classification (Kim & Brunner 2017). In the field of gravitational lenses, Petrillo et al. (2017) use CNNs to recognize galaxy-scale strong gravitational lenses based on morphological classification. They found 761 strong

lens candidates in the Kilo Degree Survey (KiDS) and after manual selection they presented 56 most reliable candidates.

However, the CNNs has not been applied for the searching of gravitational candidates based on the spectroscopic-selection technique. In this paper, we will use the Deep Residual Network (ResNet, one popular model of CNNs) to search for the galaxy-LAEs lens candidates by recognizing the Ly α emissions from the redshift of $2 < z < 3$ in the DR12 of SDSS. LAEs is a kind of young, low-mass galaxies with extremely star-formation. They are an important component of the early universe, and are critical for studying the formation and evolution of the galaxies at that time. Benefited from the magnifying effect of the gravitational lenses, galaxy-LAEs lenses can provide us good opportunities to study the LAEs themselves. More importantly, galaxy-LAEs lenses can help us to exploit the small-scale dark substructure around the lens galaxies and constrain the slope and normalization of the substructure-mass function.

The paper is organized as follows. In Section 2, we will provide a brief description of CNNs and ResNet. In Section 3, we will talk about how to use ResNet to recognize emissions that are not from the foreground galaxies themselves. In this section, we also apply our algorithm to the spectra data in the DR12 of SDSS and then compare our results with previous work (Shu et al. 2016a). In Section 4, we will present 6 new gravitational lens candidates found by our ResNet model. In Section 5, we will discuss the advantages and the possible improvement of our strategy.

2 CNNs AND RESNET

Recent years, CNNs have gained a lot of attentions in image recognition, speech recognition, motion analysis, nature language processing as well as many other researching fields. CNNs are a kind of deep feedforward neural networks with multiple different layers. The layers mainly contain the convolution layers, the pooling layers and the fully-Connected layers. The convolution layers perform convolution operation, it uses convolution kernel (or convolution neurons) to extract different feature of the input. The Pooling layers can compress the feature maps and simplify the calculations. The fully-connected layers turn all the local feature maps into a global feature map. There are lots of feature maps in each layers and each feature map can extract one feature using the convolution neurons. Usually, a feature map has several convolution neurons and the convolution neurons are composed of weights and bias which could be trained using the train data. During the training process, every convolution neuron can accept some inputs and do some convolution calculation. Figure 1 shows a simple but complete CNN with two convolution layers, two Pooling layers and one fully-connected layers. The input image is convoluted by 3 convolution kernel and yield 3 feature maps. Then these 3 feature maps are compressed by a pooling layer. After another one convolution layer and one pooling layer, a fully-connected layer is given to turn local feature maps into a global feature map.

A deep CNN model could be designed as a classifier or to achieve a regression tasks. Many evidences shows that the network depth is very important for the results of the classification and the regression tasks. Theoretically, the train

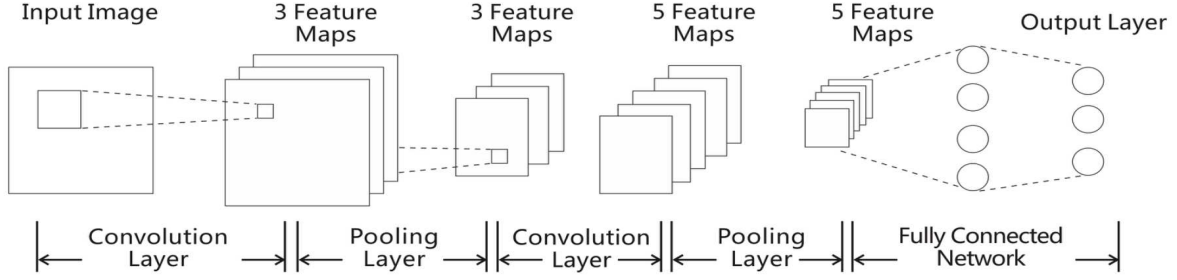


Figure 1. A simple but complete CNN with two convolution layers, two Pooling layers and one fully-Connected layers.

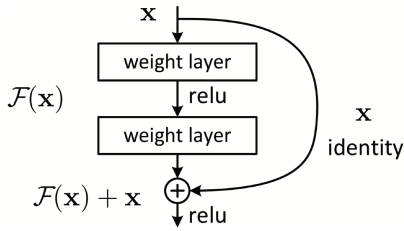


Figure 2. Residual learning: a building block with a shortcut connection (He et al. 2015). The weight layer is a assemble of several convolution layers and other necessary layers. Rule is one kind of Activation Function which limits the output signal to a finite value (Gulcehre et al. 2016).

result should become better when the layers become deeper. However, for deeper networks, when they start converging, a “degradation” problem would occurs: with the increase of network depth, accuracy gets saturated and then degrades rapidly (He et al. 2015), which is not caused by over fitting. That’s why many popular CNNs models have only a few layers (e.g., LeNet has 5 layers, Lecun et al. (1998); AlexNet has 7 layers, Krizhevsky et al. (2012)). In order to overcome the degradation of the accuracy with network depth increasing, He et al. (2015) proposed a new CNNs model: the Deep Residual Network (ResNet).

ResNet assumes that it is easier to optimize the residual mapping than to optimize the origin, unreferenced mapping. Denoting the desired underlying mapping as $H(x)$ which would be fitted by a few stacked layers, and x is the inputs of the first of these layers. ResNet lets the stacked layers to fit the residual mapping of $F(x) := H(x) - x$. Then the original mapping $H(x)$ becomes $F(x) + x$, and it could be realized by feedforward neural networks with “shortcut connections” (see Figure 2) which simply perform the identity mapping, then skip one or more layers and add their outputs to the outputs of the stacked layers. In He et al. (2015), the authors explained that “With the residual learning reformulation, if identity mappings are optimal, the solvers may simply drive the weights of the multiple nonlinear layers toward zero to approach identity mappings.”

In our study, we try to use Machine Learning (ML) to find gravitational candidates based on spectroscopic-selection technique. Spectrum is one dimensional sequence and has local correlation. Therefore, we use one dimensional CNNs to built the model, because CNNs shows good per-

formance in distinguishing the input with local correlation. We also want to guarantee the accuracy of our selections by increasing the depth of the CNN models, therefore, we adopt the ResNet model to prevent “degradation” problem and reduce the difficulty of training. In fact, before the final choice of ResNet, we have tried several “plain” networks (e.g., LeNet; AlexNet), but they are difficult to convergence in our work.

3 USE RESNET TO FIND EMISSION LINES FROM A DIFFERENT REDSHIFT

So far, several gravitational lens surveys based on spectroscopic-selection have been achieved (e.g., the SLACS, BELLS, S4TM and BELLS GALLERY). The SLACS, BELLS and S4TM surveys concentrated on searching for multiple emissions (meanly the [OII] 3727 or [OIII] 5007 emissions) from the galaxies with higher redshift than the foreground galaxies, while the BELLS GALLERY focused on just one higher redshift $\text{Ly}\alpha$ emission. In our study, we aim to use ResNet to find some galaxy- $\text{Ly}\alpha$ emitter lens candidates in the BOSS spectra by searching for high redshift ($2 < z < 3$) $\text{Ly}\alpha$ emissions in the spectra of middle redshift galaxies. We don’t search the multiple [OII] 3727 or [OIII] 5007 emissions as SLACS have done because using just one emissions to build the train/test data is more simple. However, in the band ($3800\text{\AA} < \lambda < 5000\text{\AA}$, see it in Section 3.2) we choose, the spectra with lower redshift [OII] 3727 or other emissions could also be found by our network. We will abandon these spectra through several other subsequent selections (see it in Section 4).

3.1 the BELLS GALLERY survey

The lens candidates of BELLS GALLERY are selected from the DR12 of the BOSS of the SDSS-III by searching for $\text{Ly}\alpha$ emission lines from higher redshift $\text{Ly}\alpha$ emitters, and then following up high-resolution Hubble Space Telescope (HST) imaging observations to confirm the lens nature. In Shu et al. (2016a), the first and most important step is selecting out the spectra with emissions not from the target galaxies themselves. To do this, they confined their research to the observed wavelength range of $3600\text{\AA} < \lambda < 4800\text{\AA}$ (roughly $2 < z < 3$ for the $\text{Ly}\alpha$ emissions) and used an error-weighted matched-filter with a Gaussian kernel to search the

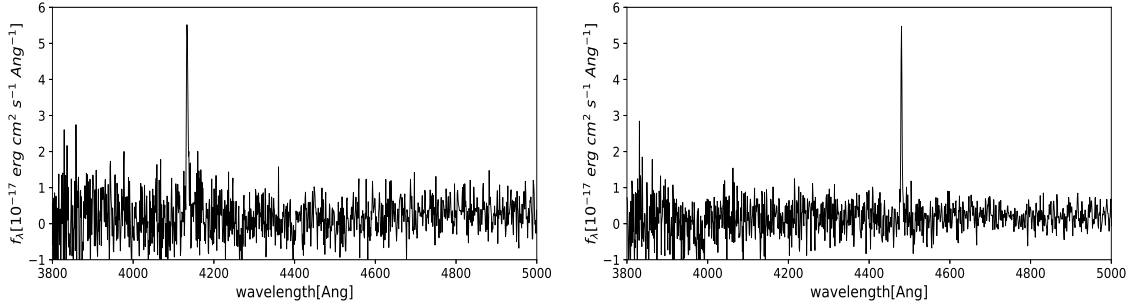


Figure 3. The left is the spectrum of SDSSJ 1110+2808 which comes from BELLS GALLERY. The right is an artificial one. Both have high SNR Ly- α lines.

Ly α emissions in BOSS targets. This mean step yielded 4982 hits. Then they performed several subsequent selections to reject the false hits and finally found 187 lens candidates with obvious Ly α emissions from higher redshift. They presented 21 highest quality BELLS GALLERY candidates in their paper, and among them 17 candidates have been confirmed to be strong gravitational lenses by HST imaging observations. The goal of the BELLS GALLERY survey is to exploit the small-scale dark substructure around ETGs and to constrain the slope and normalization of the substructure-mass function.

BELLS GALLERY is a successful lens candidates searching work. However, the first step of the selections is complex and consume too much time. First, they have to obtain an accurate estimate of the spectroscopic flux errors across the observed spectra; second, a standard spectroscopic template for ETGs is needed to fit each spectrum and obtain the galaxy-subtracted residual spectrum. For millions of targets, these procession would consume too much time. Therefore, in order to improve the selection speed of this step, we introduce ResNet to automatically select out the spectra with emissions which are not from the targets themselves.

3.2 the predictive data and the train/test data

We aim to use ResNet to search for galaxy-LAEs lens candidates from the DR12 of BOSS of SDSS-III based on spectroscopic-selection. Firstly, we need to filter out all the ETGs spectra from the database to build our predictive data. The BOSS targets have been classified as several classes, such as "GALAXY", "SKY", "STAR". Therefore, we can choose the "GALAXY" class and reject the targets with subclass keyword of "STARFORMING", "BROADLINE" and "AGN". We then limit our selection to the redshift range of $z > 0.3$. These selections result in 1,241,799 recorders. For these recorders, we cut out the part ranged from 3800Å to 5000Å of each spectrum to build our predictive spectra. Notice that we don't use the same wavelength range as BELLS GALLERY ($3600\text{Å} < \lambda < 4800\text{Å}$), because we find that the wavelength ranged from 3600Å to 3800Å is very noised, which could decrease the accuracy of our ResNet model.

Our predictive data includes 177 known lens candidates from Shu et al. (2016a), the remaining 10 candidates in their work are eliminated because of the redshift limitation. Ad-

ditionally, the Ly α emissions of 3 of the 177 candidates fall out the wavelength of $3800\text{Å} < \lambda < 5000\text{Å}$. Therefore, if we use this known lens candidates to test our ResNet model, only 174 candidates could be used.

Finding lens candidates in a great deal of galaxy spectra is an classification problem. Therefore, we use ResNet to build a classifier which can select out the spectra with emissions not from the foreground galaxies themselves, and then use several other subsequent selections similar with previous work to reject the false hits. The quality of the train/test data is very critical for the accuracy of the classifier and directly affect the efficiency of the selection. For the train/test data, we require: 1.) the train/test data is not in the DR12 of the BOSS of SDSS-III database, but looks similar as the spectra in it; 2.) the number of the train/test spectra have to be enough, usually more than ten thousands; 3.) the train/test data are classified to two groups, one group has no Ly α emissions (labeled [0]), and the other one has Ly α emissions (labeled [1]); 4.) for the real spectra in DR12, the spectra with Ly α emissions are much less than the spectra without Ly α emissions, which makes serious data imbalance, therefore, a similar data imbalance should exists in the train/test data.

So far, we just have no more than 200 galaxy spectra with Ly α emissions from higher redshift, which is far from enough. Therefore, we use the following procedure to build an artificial train/test data set.

(i) We grid the redshift to small bins ($\delta z = 0.0025$) and perform a Principal Component Analysis (PCA) to the spectra of ETGs (Chen et al. 2012; Shu et al. 2012) at each redshift bin. Then we use the first six eigenvectors of the PCA to create some artificial galaxy spectra at the corresponding redshift bin. This procedure yields totally 150,000 artificial galaxy spectra.

(ii) We add the "sky" and "noise" (from BOSS targets) to the created spectra and now the galaxy spectra looks similar as real spectra. We then cut out the part ranged from 3800Å to 5000Å of each spectrum.

(iii) In the rest-frame wavelength, we crate 10,000 artificial Ly α emissions using Gaussian profiles. The mean wavelength of the Gaussian profiles is at 1216Å and the Full Width at Half Maximum (FWHM) is randomly obtained from a normal distribution with the mean value of $300\text{km}\cdot\text{s}^{-1}$ and standard deviation of $200\text{km}\cdot\text{s}^{-1}$. We then limit the FWHM greater than 0.5Å and the peak of the emissions greater than $1.5 \times 10^{-17}\text{erg}\cdot\text{cm}^2\cdot\text{Ang}^{-1}$. Finally, we ran-

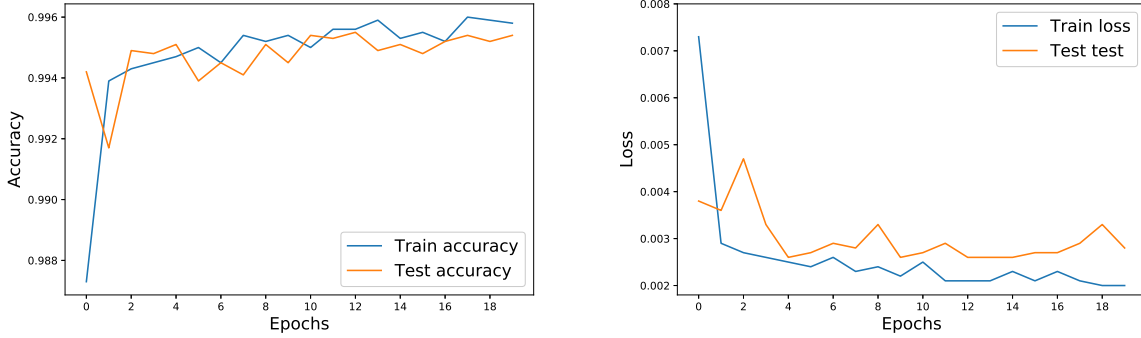


Figure 4. The left figure is the train/test accuracy while the right is the corresponding loss.

domly shift the emissions to the wavelength of $3800\text{\AA} < \lambda < 5000\text{\AA}$

(iv) We randomly select 10,000 spectra from the totally 150,000 spectra and add the 10,000 artificial $\text{Ly}\alpha$ emissions to them, then label them [1]. The remaining spectra without emissions are labeled [0]. The spectra with $\text{Ly}\alpha$ emissions are 1/15 of the total train/test spectra in order to overcome the data imbalance we mentioned above.

Now, we have successfully built 150,000 train/test spectra. The PCA approach we performed in the first step will loss some information of the spectra. However, we point out that the lost information does not affect our training and results. Because, firstly the first 6 eigenvectors are enough to fit a real spectrum with an acceptable χ^2 ; secondly, most of the lost information is the noise, after we add the “sky” and “noise” in the second step, the created spectra looks the same as real spectra. Figure 2 shows two high Signal-to-Noise Ratio (SNR) spectra with $\text{Ly}\alpha$ emissions. The left one is the real spectrum of SDSS J1110+2808 (one of BELLS GALLERY samples), while the right is an artificial one with an synthetical $\text{Ly}\alpha$ emission. They are look very similar. Another point we need to discuss is the Gaussian profile approximations for creating $\text{Ly}\alpha$ emissions. As we will show in Section 4, the $\text{Ly}\alpha$ emission is in fact skewed. However, in this study, we just want to use ResNet to recognise the emissions with any shapes. The shape judgement will be done by some other subsequent selections. Therefore, using skewed profiles to create $\text{Ly}\alpha$ is not needed. During the test, we find the Gaussian profile approximations can efficiently find the emissions with any shapes.

3.3 Our ResNet model

Our ResNet model has 8 blocks, 28 Convolution Layers, which is much deeper than plain CNNs. We add a “Max-pooling” layer between any two blocks. A Dropout layer is employed before the fully connected layer to prevent overfitting. As mentioned before, the samples labeled [1] are far less than the samples labeled [0], making a serious data imbalance. Here, we also add another measure—using the “Focal Loss” to overcome the effect of the data imbalance. The “Focal Loss” can be written as

$$L_{fl} = \begin{cases} -(1 - \hat{y})^y \log \hat{y} & \text{when } y = 1 \\ -\hat{y}^y \log(1 - \hat{y}) & \text{when } y = 0 \end{cases} \quad (1)$$

Where $y \in \{0, 1\}$ is the real label while \hat{y} is the prediction value. The “Focal Loss” is designed to improve the classifying task with extreme data imbalance, which is described detailedly in Lin et al. (2017).

Next, we apply our program to the train/test data (The ratio of the train and test data is 9 : 1). In the training process, we mask the location of [NeV] 3347, [NeV] 3427, [OII] 3727 and [NeIII] 3869 emissions, which may come from the ETGs themselves. The output of our program for each spectrum is the probability to be a lens candidate. We treat the samples with probability greater than 0.5 as lens candidates. Figure 3 shows the accuracy and loss of the train/test data. We obtain a near-perfect test accuracy of 0.9954, and the corresponding loss is 0.0028. After successfully training the ResNet model, we apply the model to our predictive data (The emissions of the ETGs themselves also have been masked). We find all the 21 BELLS GALLERY lens candidates with the possibilities extremely close to 1. For all the 174 known lens candidates in our predictive spectra, we find 161 of them. The discovery rate is 92.5%.

4 NEW STRONG GRAVITATIONAL LENSING CANDIDATES

We find 1232 hits using our ResNet model, including 161 candidates which have been found in Shu et al. (2016a). Apart from the hits exist in the 4982 hits of BELLS GALLERY, we also find 536 hits. Next, we perform several subsequent selections used by Shu et al. (2016a) to remove the false hits. In order to ensure the higher quality, we first apply a visual inspection to the 536 hits and reject the samples with too much noise and very lower emission lines (the peak value of the emission flux is about less than $1 \times 10^{-17} \text{ erg} \cdot \text{cm}^2 \cdot \text{Ang}^{-1}$). This cut left 124 hits. For these 124 hits, we remove the hits with significant numerical over-densities in both observed wavelength (associated with airglow features, see it in Shu et al. (2016a)) and BOSS target-galaxy rest wavelength (associated with template-subtraction residuals). This step remove 77 spurious hits. One typical feature of high redshift $\text{Ly}\alpha$ emissions is the “blue edge, red tail” profiles (see it in BELLS GALLERY samples). Therefore, we use the skew normal profiles plus a horizontal line to fit the emissions of the remained 47 hits and finally left 22 samples with skewness parameter bigger

Table 1. Selected properties of the 6 galaxy-LAE lens candidate systems.

Target	Plate-MJD-Fiber	z_L	z_s	R.A.	Decl.	m_i	Ly α Flux
SDSS J111749.50+014036.9	4731-55656-197	0.5840	2.1570	11:17:49.50	+01:40:36.95	19.35	30.4
SDSS J121650.13+500700.2	6671-56388-589	0.6613	2.7894	12:16:50.13	+50:07:00.26	19.83	36.7
SDSS J122502.89-000907.8	3847-55588-309	0.4868	2.4395	12:25:02.89	-00:09:07.85	19.61	12.3
SDSS J142310.55+231928.1	6013-56074-66	0.4717	2.4099	14:23:10.55	+23:19:28.17	19.66	50.8
SDSS J143428.11+470111.5	6736-56366-505	0.5070	2.3913	14:34:28.11	+47:01:11.53	19.25	24.2
SDSS J153520.91+235221.7	3948-55331-685	0.4945	2.9754	15:35:20.91	+23:52:21.79	19.3	7.2

NOTE. — Column 1 is the SDSS system name in terms of truncated J2000 R.A and decl. in the format HHMMSS.ss± DDMMS.s. Column 2 provides the plate-MJD-fiber of the spectra. Columns 3 and 4 are the redshifts of the foreground lenses and the background galaxies inferred from the BOSS spectra. Column 5 and 6 is the coordinate in terms of truncated J2000 R.A and decl. Column 7 is the BOSS-measured i -band apparent cmodel magnitude within the 1'' fiber. And column 8 is the total apparent flux of the Ly α emission in units of $10^{-17} \text{ erg} \cdot \text{cm}^{-2} \cdot \text{s}^{-1}$.

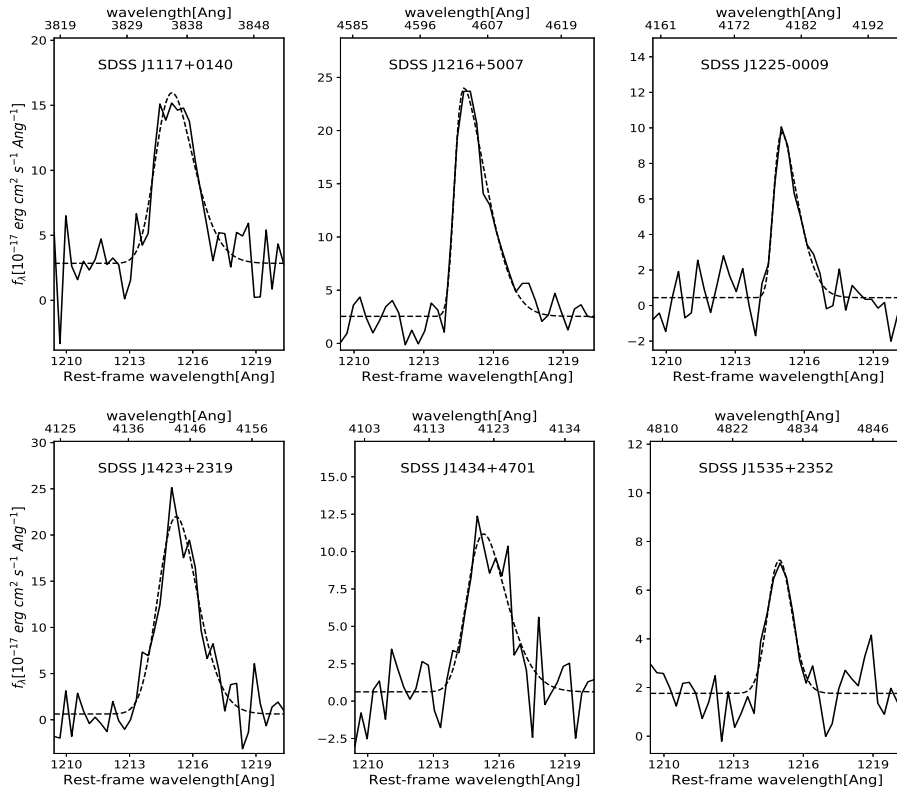


Figure 5. Zoomed in views of the Ly α emission lines for the candidates ordered by decreasing apparent Ly α flux, de-redshifted to the rest frame of the LAEs. Dashed lines are the best-fit continuum flux for the Ly α emissions using skew normal distribution. Note the line profiles with "blue edge" and "red tail" are the characteristic of LAEs.

than 0. This fitting is achieved by non-linear least squares. During the fitting process, we use 4 parameters (the Skewness, Mean Value, Standard Deviation and Kurtosis) to describe the skew normal profiles and 1 parameter (Height) to describe the horizontal line which represents the stationary noise. All these 5 parameters are varied. We then remove 16 samples with low-redshift [OII] emissions. In this step, we suppose the emissions are [OII] emissions and calculate the relative positions of OIII, H α and H β emissions. If any of these positions has an emission, we reject the sample. Finally, we obtain 6 LAEs lens candidates and their properties are shown in Table 1. We also show the emission profiles and their best fitting skew normal profiles in Figure 4. For the 6 lens candidates, the Ly α emission of 1 sample (SDSS

J153520.91+235221.7) falls into the redshift range of $4800\text{\AA} < \lambda < 5000\text{\AA}$, which is higher than BELLS GALLERY samples.

5 DISCUSSION AND IMPROVEMENT

Comparing with Shu et al. (2016a), we find an equal number of galaxy-LAEs lens candidates (161+6) in the same database (DR12 of BOSS) using Machine Learning. However, the recognition speed of our strategy is much higher than that of theirs. After successfully training the model, we can finish the recognition process within just an hour and a half using the Central Processing Unit (CPU) of a common

laptop computer. By contrast, the method used in [Shu et al. \(2016a\)](#) needs about 10 hours to finish a similar recognition. Graphic Processing Unit (GPU) can effectively increase the recognition speed, usually 5 to 10 times compared with CPU. Although we have not tried the GPU computation, we can expect that the recognition could be finished within 20 minutes. This speed advantage would become important with the arrival of the big data age of astronomy. It is noted that our recognition process doesn't include the training process. Although we have to spend several hours to train the network in the beginning, our strategy is still a high efficient one, because after the network has been successfully trained, it can be used to any other predictive data without retraining.

This work is the first attempt to find lens candidates with ResNet based on spectroscopic-selection. Our strategy still has very large development space. The first problem to overcome is the noise. During the repeating experiments, we find the spectra with too much noise could decrease the accuracy, therefore we reject the wavelength range of $3600\text{\AA} < \lambda < 3800\text{\AA}$. The second problem is the subsequent selections. Our ResNet can successfully find the spectra with emissions from a different redshift, but it can not judge whether they are $\text{Ly}\alpha$ emissions from higher redshift or [OII] emissions from lower redshift. Therefore, after the ResNet selection, several subsequent selections used in previous work is needed. If we want to use ResNet to directly find the emissions with skewness bigger than 0, building the emissions with skewed profile and classifying the train data to 3 class is an approach. The first class is the spectra with no emissions, the second is the spectra with skewed emissions which have negative skewness and the third is the spectra with skewed emission which have positive skewness. However, this approach still needs subsequent selections and seems unnecessary in this work. An alternative method is to use a regression ResNet model to give the redshift of the source galaxies. This method requires the whole spectrum. We hope the regression model could learn the redshift of the source through the relative position of multiple emissions. However, to overcome the data imbalance, a regression model is more difficult than a classification model.

6 CONCLUSIONS

In this work, we have applied the ResNet model to search for galaxy-LAEs lens candidates in DR12 of the BOSS of SDSS-III based on spectroscopic-selection. We use 140,000 spectra without $\text{Ly}\alpha$ emissions and 10,000 ones with $\text{Ly}\alpha$ emissions to train a 28 layers ResNet model and get a near-perfect test accuracy of 0.9954 with the corresponding loss of 0.0028. After we apply our ResNet model to the 1,241,799 predictive spectra from the DR12 of the BOSS of SDSS-III, we find 1232 hits, including 161 known lens candidates. For all the 187 known candidates in [Shu et al. \(2016a\)](#), there are only 177 spectra in our predictive data and the $\text{Ly}\alpha$ emissions of 3 candidates fall outside the wavelength range of $3800\text{\AA} < \lambda < 5000\text{\AA}$. We actually find 92.5% of the known candidates. Finally, we perform several subsequent selections to new 536 hits and find 6 new galaxy-LAEs lens candidates. The most obvious advantage of our strategy is the recognition speed. Comparing with previous work ([Shu et al. 2016a](#)), we find

a similar number of lens candidates in the same database with much less time. This work is just the first attempt to find lens candidates using Machine Learning. We will continue to improve the strategy and build a perfect method to search galaxy-scale lens candidates.

7 ACKNOWLEDGEMENT

We acknowledge the financial support from the National Natural Science Foundation of China 11573060 and 11661161010. Y.S. has been supported by the National Natural Science Foundation of China (No. 11603032 and 11333008), the 973 program (No. 2015CB857003), and the Royal Society - K.C. Wong International Fellowship (NF170995).

REFERENCES

- Auger M. W., Treu T., Bolton A. S., Gavazzi R., Koopmans L. V. E., Marshall P. J., Bundy K., Moustakas L. A., 2009, *ApJ*, 705, 1099
- Auger M. W., Treu T., Bolton A. S., Gavazzi R., Koopmans L. V. E., Marshall P. J., Moustakas L. A., Burles S., 2010, *ApJ*, 724, 511
- Bolton A. S., Burles S., Schlegel D. J., Eisenstein D. J., Brinkmann J., 2004, *AJ*, 127, 1860
- Bolton A. S., Burles S., Koopmans L. V. E., Treu T., Moustakas L. A., 2006, *ApJ*, 638, 703
- Bolton A. S., Burles S., Koopmans L. V. E., Treu T., Gavazzi R., Moustakas L. A., Wayth R., Schlegel D. J., 2008, *ApJ*, 682, 964
- Bolton A. S., et al., 2012, *ApJ*, 757, 82
- Brownstein, J. R., Bolton, A. S., Schlegel, D. J., et al. 2012, *ApJ*, 744, 41
- Dawson K. S., et al., 2013, *AJ*, 145, 10
- Dieleman S., Willett K. W., Dambre J., 2015, *MNRAS*, 450, 1441
- Eisenstein, D. J., Weinberg, D. H., Agol, E., et al. 2011, *AJ*, 142, 72
- Gavazzi R., Marshall P. J., Treu T., Sonnenfeld A., 2014, *ApJ*, 785, 144
- Gehring J., Auli M., Grangier D., Yarats D., Dauphin Y. N., 2017, *arXiv*, arXiv:1705.03122
- Gulcehre C., Moczulski M., Denil M., Bengio Y., 2016, *arXiv*, arXiv:1603.00391
- Hála P., 2014, *arXiv*, arXiv:1412.8341
- He K., Zhang X., Ren S., Sun J., 2015, *arXiv*, arXiv:1512.03385
- Horesh A., Ofek E. O., Maoz D., Bartelmann M., Meneghetti M., Rix H.-W., 2005, *ApJ*, 633, 768
- Hoyle B., 2016, *A&C*, 16, 34
- Impellizzeri C. M. V., McKean J. P., Castangia P., Roy A. L., Henkel C., Brunthaler A., Wucknitz O., 2008, *Natur*, 456, 927
- Joseph, R., Courbin, F., Metcalf, R. B., et al. 2014, *A&A*, 566, A63
- A. Krizhevsky, I. Sutskever, and G. Hinton. Advances in neural information processing systems, page 1097–1105. (2012)
- Lenzen F., Schindler S., Scherzer O., 2004, *A&A*, 416, 391
- Lecun, Y. & Bottou, L. & Bengio, Y. & Haffner, P. (1998). Proceedings of the IEEE. 86. 2278 - 2324. 10.1109/5.726791.
- Lin T.-Y., Goyal P., Girshick R., He K., Dollár P., 2017, *arXiv*, arXiv:1708.02002
- Kim E. J., Brunner R. J., 2017, *MNRAS*, 464, 4463
- Kubo J. M., Dell'Antonio I. P., 2008, *MNRAS*, 385, 918
- Koopmans L. V. E., Treu T., 2003, *ApJ*, 583, 606

- Koopmans L. V. E., Treu T., Bolton A. S., Burles S., Moustakas L. A., 2006, *ApJ*, 649, 599
- Koopmans, L. V. E., Bolton, A., Treu, T., et al. 2009, *ApJ*, 703, L51
- Meyer R. A., Delubac T., Kneib J.-P., Courbin F., 2017, *arXiv*, [arXiv:1711.01184](#)
- More A., Cabanac R., More S., Alard C., Limousin M., Kneib J.-P., Gavazzi R., Motta V., 2012, *ApJ*, 749, 38
- Petrillo, C. E., Tortora, C., Chatterjee, S., et al. 2017, *MNRAS*, 472, 1129
- Ruff A. J., Gavazzi R., Marshall P. J., Treu T., Auger M. W., Brault F., 2011, *ApJ*, 727, 96
- Shu Y., Bolton A. S., Schlegel D. J., Dawson K. S., Wake D. A., Brownstein J. R., Brinkmann J., Weaver B. A., 2012, *AJ*, 143, 90
- Shu, Y., Bolton, A. S., Brownstein, J. R., et al. 2015, *ApJ*, 803, 71
- Shu, Y., Bolton, A. S., Kochanek, C. S., et al. 2016, *ApJ*, 824, 86
- Shu, Y., Bolton, A. S., Mao, S., et al. 2016, *ApJ*, 833, 264
- Suyu, S. H., Auger, M. W., Hilbert, S., et al. 2013, *ApJ*, 766, 70
- Seidel G., Bartelmann M., 2007, *A&A*, 472, 341
- Sonnenfeld A., Treu T., Gavazzi R., Suyu S. H., Marshall P. J., Auger M. W., Nipoti C., 2013, *ApJ*, 777, 98
- Swinbank, A. M., Webb, T. M., Richard, J., et al. 2009, *MNRAS*, 400, 1121
- Treu T., Koopmans L. V. E., 2004, *ApJ*, 611, 739
- Treu T., Dutton A. A., Auger M. W., Marshall P. J., Bolton A. S., Brewer B. J., Koo D. C., Koopmans L. V. E., 2011, *MNRAS*, 417, 1601
- Treu, T., Schmidt, K. B., Brammer, G. B., et al. 2015, *ApJ*, 812, 114
- Warren S. J., Hewett P. C., Lewis G. F., Møller P., Iovino A., Shaver P. A., 1996, *MNRAS*, 278, 139
- Chen, Y.-M., Kauffmann, G., Tremonti, C. A., et al. 2012, *MNRAS*, 421, 314